

# The Bauschinger Effect Magnitude Control in Ultra-Low Carbon Steel Wires

Felipe Farage David<sup>a,b\*</sup> , Rafael de Oliveira Cordeiro<sup>b</sup>, Luan Marcel Costa Vasconcelos<sup>a</sup> ,  
Ben Dêvide de Oliveira Batista<sup>c</sup> , Frank de Mello Liberato<sup>b</sup>, Adilson Rodrigues da Costa<sup>a</sup> 

<sup>a</sup>Universidade Federal de Ouro Preto, Rede Temática em Engenharia de Materiais – REDEMAT, Praça Tiradentes, 20, 35400-000, Ouro Preto, MG, Brasil.

<sup>b</sup>Instituto Federal de Educação, Ciência e Tecnologia de Minas Gerais, Avenida Michael Pereira de Souza, 3007, 36417-050, Campinho, Congonhas, MG, Brasil.

<sup>c</sup>Universidade Federal de São João Del-Rei, Rodovia 443, km 7, 36307-352, Ouro Branco, MG, Brasil.

Received: September 12, 2022; Revised: January 04, 2023; Accepted: January 09, 2023

The cold roller die process increases the tensile strength and decreases the ductility of steel wire. Annealing heat treatment is applied to restore mechanical properties, but this is a costly process. This research shows that it is possible to control the mechanical properties of ultra-low carbon steel wire inducing the Bauschinger effect and relieving residual steel stresses. The present study uses several pulleys to promote and control the Bauschinger effect magnitude through alternated cyclic bending. A Completely Randomized Design, a regression study, and the Akaike Information Criterion were used to understand the relationship between the quantity and diameter of pulleys and the influence on the magnitude of the Bauschinger effect. Statistical models showed that it is possible to have a maximum increase of 103% in uniform elongation and a maximum decrease of 14% in yield strength. An interaction between the factors studied in controlling the Bauschinger effect magnitude was confirmed.

**Keywords:** *Bauschinger effect, Ultra-low carbon steel wire, Stress relief, Completely Randomized Design in factorial scheme, Akaike Information Criterion, Response Surface Methodology.*

## 1. Introduction

The cold forming process increases the strength and decreases the ductility of metals. Typical examples are roller die and conventional wire drawing processes<sup>1</sup>. Thermally activated processes, such as the annealing heat treatment, are usually used to restore the mechanical properties of steel. However, heat treatments are costly and have a significant environmental impact due to burning fossil fuels (such as natural gas) or using liquid lead as thermal energy sources to heat the wire<sup>2</sup>. Consequently, there is a growing demand for more sustainable, environmentally friendly, and cost-effective alternatives for stress-relieving steel wires. Alternatively, this work propose to promote microstructural softening by controlling the Bauschinger effect in alternate bending cycles.

The Bauschinger effect occurs when a metal or metal alloy is cyclically loaded, increasing the ductility and decreasing the strength of materials<sup>3,4,5,6</sup>. Several studies have been developed to explain this phenomenon. High-resolution microscopic scale observations confirm that the metal plasticity recovery occurs due to the dislocations rearrangement into a sub-grain structure and, in some cases, due to the reduction of the dislocation density by mutual annihilation<sup>7</sup>.

This phenomenon is considered harmful for most steels<sup>8,9,10</sup>, since these mechanical property changes occur without their magnitude being controlled. In contrast, once the intensity of this phenomenon is controlled, it is possible

to use it to adjust the final steel mechanical properties, such as yield strength, tensile strength, and uniform elongation.

Several techniques have been applied to promote the Bauschinger effect in metals, of which the most usual are the cyclic tension-compression<sup>11,12,13</sup>, cyclical torsion<sup>14,15,16</sup> and cyclical bending<sup>7,17</sup>. In all of these mentioned techniques the cyclic loading is applied to the metal. So, from cycle to cycle, the yield stress, which determines the entry into the plastic regime, gradually decreases. Similar effects usually occur when a significant change in the plastic deformation path occurs, characterizing the Bauschinger effect<sup>18,19,20</sup>.

Among the mentioned techniques, those that require the promotion of cyclic loading by uniaxial tensile-compressive and by cyclical torsion are challenging to implement in a large-scale production line. On the other hand, cyclical bending is quite common in industrial practice and can be observed in the coiling, uncoiling, and straightening of plates and long steel products<sup>27</sup>. Thus, cyclical bending can be implemented at the end of the roller die production line or wire drawing process to reasonably restore the plasticity of the metal.

However, to effectively implement this system in the industrial sector, it is necessary to build models that describe the strength and plasticity variation as a function of the operational parameters of cyclic bending as number and/or diameter of pulleys. For this purpose, Akaike Information Criterion (AIC)<sup>21</sup> is an essential criterion for model selection. A model selection is a fundamental step since an under-fitted

\*e-mail: felipe.farage@ifmg.edu.br

**Table 1.** Chemical composition (wt.%) of steel wire.

Element	C	Mn	Si	P	S	Ti	Nb
Composition (wt.%)	0.002	0.20	0.0	0.009	0.006	0.012	0.013

model might not capture the true nature of the variability in the response variable and, consequently, will tend to have a low-quality predictive performance. In contrast, an over-fitted model loses generality and contains more parameters than those that can justify by the experimental data<sup>22</sup>. Hence, AIC is an efficient predictor of fit quality, selecting the best model that balances these drawbacks. First, an analysis of variance (ANOVA) in conjunction with regression analysis is performed to determine the significance between coefficients of the predictor variables (number of pulleys and pulley diameter) and the outcome desired (wire diameter, yield strength, tensile strength, and uniform elongation).

This paper contributes to the comprehension of the steel wire macroscopic stress-strain state after applying cyclic bending and discusses the related strength variations. So, the objective was to analyze the efficiency of cyclic bending on the mechanical strength of the ultra-low carbon steel wire to control the Bauschinger effect magnitude. This study controlled the intensity of plastic recovery of steels subjected to high rates of cold strain. Industrially, this effect control can modify the strength and plasticity of wire, creating possibilities to propose new production paths with environmental and productive sustainability improvements and cost reductions. The originality of this work is highlighted by the application of cyclic bending to control the magnitude of the Bauschinger effect in steel wires, using equations, surface response and contour plots as well.

## 2. Materials and Experimental Methods

An ultra-low carbon steel wire with a 1.255 mm diameter and 95% cold reduction was chosen for the experiments. The chemical composition, in weight percentage, is shown in Table 1. The mechanical properties obtained by tensile testing are presented in Table 2. It is noticeable that the wire exhibits a high level of strain hardening since the uniform elongation is relatively low.

The alternated cyclical bending was performed at room temperature with a constant processing speed of 200 mm/s. The pulleys were placed in fixed positions, always maintaining a symmetrical sinusoidal deformation path, as shown in Figure 1. During the cyclical bending, the wire was pulled by a 365 mm diameter coiler.

The experimental statistical methodology followed a Completely Randomized Design (CRD) in a double factorial scheme<sup>23</sup>. The predictor variables used were the number of pulleys (4, 8, 12, 16 and 20) and the diameter of the pulleys (Figure 2) (D1 = 28 mm, D2 = 59 mm and D3 = 85 mm), amounting to 15 parameter combinations.

The mechanical properties (yield strength at which the permanent elongation is 0.2%, tensile strength and uniform elongation) have been measured after 15 experimental conditions through tensile testing, using three samples each. An EMIC universal testing machine (Instron Company), model DL, with a load cell of 100 kN capacity, was used to perform these tests. The adopted parameters for the tensile

**Table 2.** Ultra-low carbon steel wire mechanical properties.

Diameter (mm)	Yield Strength (MPa)	Tensile Strength (MPa)	Uniform Elongation (%)
1.255	610.3	645.0	1.18

**Table 3.** Representation of the 12 linear models of the possible interactions between the independent variables.

Model	Equation
M1	$Z = \beta_0 + \beta_1 N + \beta_2 D + \epsilon$
M2	$Z = \beta_0 + \beta_1 N + \beta_2 N^2 + \beta_3 D + \epsilon$
M3	$Z = \beta_0 + \beta_1 N + \beta_2 D + \beta_3 D^2 + \epsilon$
M4	$Z = \beta_0 + \beta_1 N + \beta_2 N^2 + \beta_3 D + \beta_4 D^2 + \epsilon$
M5	$Z = \beta_0 + \beta_1 N + \beta_2 D + \beta_3 N.D + \epsilon$
M6	$Z = \beta_0 + \beta_1 N + \beta_2 N^2 + \beta_3 D + \beta_4 N.D + \epsilon$
M7	$Z = \beta_0 + \beta_1 N + \beta_2 D + \beta_3 D^2 + \beta_4 N.D + \epsilon$
M8	$Z = \beta_0 + \beta_1 N + \beta_2 N^2 + \beta_3 D + \beta_4 D^2 + \beta_5 N.D + \epsilon$
M9	$Z = \beta_0 + \beta_1 N + \beta_2 N^2 + \beta_3 D + \beta_4 D^2 + \beta_5 N.D + \beta_6 N^2.D + \epsilon$
M10	$Z = \beta_0 + \beta_1 N + \beta_2 N^2 + \beta_3 D + \beta_4 D^2 + \beta_5 N.D + \beta_6 D^2.N + \epsilon$
M11	$Z = \beta_0 + \beta_1 N + \beta_2 N^2 + \beta_3 D + \beta_4 D^2 + \beta_5 N.D + \beta_6 N^2.D + \beta_7 D^2.N + \epsilon$
M12	$Z = \beta_0 + \beta_1 N + \beta_2 N^2 + \beta_3 D + \beta_4 D^2 + \beta_5 N.D + \beta_6 N^2.D + \beta_7 D^2.N + \beta_8 N^2.D^2 + \epsilon$

tests were 406 mm long specimens and a constant crosshead speed of 10 mm/min. An electronic strain gauge 25 mm long was attached to the specimen to track the strain up to the maximum stress at the uniform strain range. Test data were, as recommended, transformed into true stress and true strain data up to maximum tensile load<sup>24</sup>.

Starting from the experimental data correlated with the tensile test, 12 models were selected, which describe the possible interactions between the independent variables (number and diameter of pulleys) up to the second-order polynomial level (Table 3). Table 3 describes the models with their respective interactions, where “N” represents the number of pulleys, “D” the diameter of the pulleys, “ $\beta_i$ ” are the estimated regression coefficients for each parameter of the considered equations, “ $\epsilon$ ” is the error term, and “Z” one of the four steel wire mechanical properties after cyclical bending (wire diameter, yield strength, tensile strength, and uniform elongation).

A parsimonious model was chosen for each of the four response variables, and the Akaike Information Criterion (AIC)<sup>21</sup> was used to evaluate the quality and selection of the model. The model corresponding to the smallest value of AIC is considered the most appropriate. Once the best model was selected, the standard null hypothesis test (Fisher’s F-test) was applied to determine the significance between the coefficients of the predictor variables and the outcome of interest<sup>25</sup>. Further statistical parameters were analyzed, such as the coefficient of determination “R<sup>2</sup>”, adjusted coefficient of determination “Adj. R<sup>2</sup>”, coefficient of variation “CV”, and adequate precision “AP”.

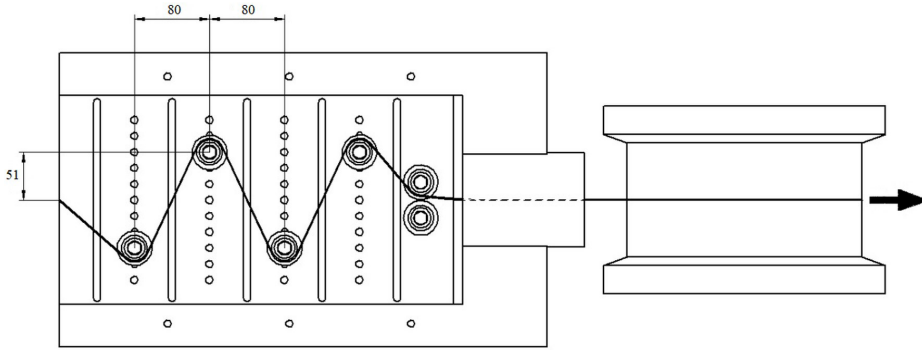


**Figure 1.** Illustration of the pulley positioning for applying cyclic bending to the wire in millimeters.

The coefficient of determination “ $R^2$ ” gives the ratio of the total variability in the experimental data, which each of the four models can explain. Therefore, a high  $R^2$  value, close to 1, is desirable in agreement with adjusted “ $R^2$ ”<sup>26,27</sup>. The statistical analysis and the graphical representation were performed in the R software environment<sup>28,29</sup>.

Based on the chosen model, according to the AIC criterion, 2D (contour plots) and 3D (response surface) graphical representation<sup>29,30</sup> of the predictor variable behavior as a function of the response variables were performed. Thus, it is possible to visualize the mechanical properties behavior as a function of the operational variables controlled in the cyclic bending process. Using this graphical representation provided by the selected models also make it possible to control the Bauschinger effect magnitude in the mechanical properties of steel wire, which is the main objective of this study. Furthermore, the optimal region, which relates the balance between maximum reduction strength and increase in plasticity, was identified based on the main parameters in the overlay plot.

### 3. Results and Discussion

#### 3.1. Experimental results and statistical analysis

The relation between the two variables controlled in cyclic bending (pulley number and pulley diameter) and the four wire properties (diameter ( $D_w$ ), yield strength ( $\sigma_y$ ), tensile strength ( $\sigma_t$ ), and uniform elongation ( $E_u$ )) were examined in two stages. First, the analysis of variance (ANOVA) was performed to verify the effect of the factors and later applied to perform multiple linear regression analysis to verify the contribution of factor levels to the response variables in the study. Table 4 shows the results of the tensile tests (yield strength, tensile strength, uniform elongation), and the wire diameter measurements for the 15 conditions tested. This table shows the mean and standard deviation results for all conditions tested (5x3 full factorial design).

Table 5 shows the AIC values for each model from Table 3 regarding the response variables after cyclic bending processing. According to this quality fit criterion, model 11 for yield strength and model 12 for wire diameter, tensile strength, and uniform elongation presented the lowest AIC values, being the most parsimonious and, therefore,

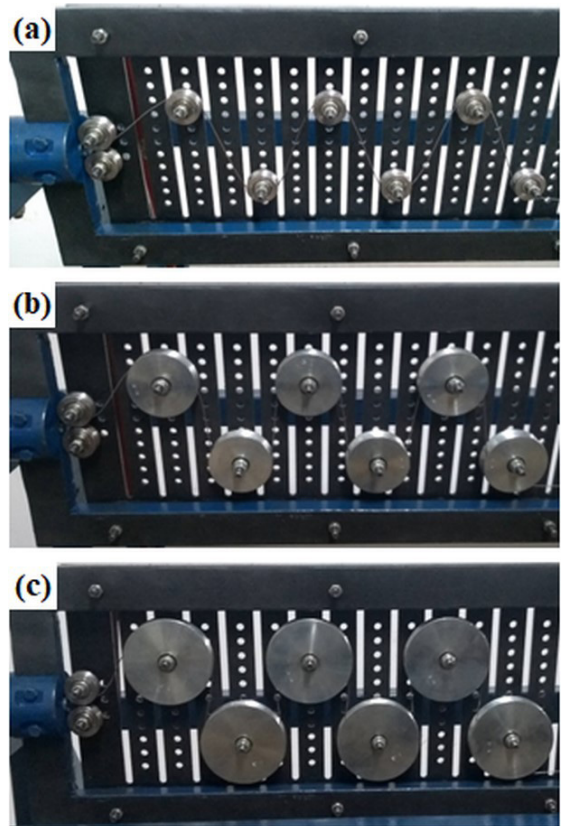


**Figure 2.** Display of the 3 size pulley inner diameters in sinusoidal positions used in the experiments: (a) 28 mm, (b) 59 mm, (c) 85 mm.

the selected ones to explain the correlation between the involved variables.

The AIC was used along with additional criteria to verify the goodness of fit of the statistical model, such as P-value, the coefficient of determination “ $R^2$ ”, the adjusted coefficient of determination “Adj.  $R^2$ ”, the coefficient of variation “CV” and adequate precision “AP” (Table 6).

The P-value in Table 6 for all models is less than 0.05, which indicates that the four models are significant in explaining the correlation between the predictor variables

**Table 4.** CRD for the study of two experimental variables and obtained results.

Run No.	Conditions		After Cyclic Bending Testing Results			
	Pulley Quantity	Pulley Diameter (mm)	Wire Diameter (mm)	Yield Strength (MPa)	Tensile Strength (MPa)	Uniform Elongation (%)
1	4	59	1.254 ± 0.001	535.8 ± 8.2	652.8 ± 2.6	2.37 ± 0.08
2	4	28	1.251 ± 0.002	529.5 ± 6.6	642.8 ± 3.9	2.07 ± 0.06
3	20	28	1.091 ± 0.002	663.0 ± 4.7	687.3 ± 1.8	0.95 ± 0.08
4	12	28	1.207 ± 0.001	555.0 ± 3.4	647.3 ± 4.0	2.05 ± 0.13
5	4	85	1.251 ± 0.001	564.5 ± 4.0	655.6 ± 1.1	1.71 ± 0.07
6	8	59	1.256 ± 0.001	531.1 ± 1.3	634.3 ± 2.7	2.01 ± 0.11
7	16	28	1.160 ± 0.003	606.4 ± 4.3	668.1 ± 3.7	1.52 ± 0.12
8	20	59	1.249 ± 0.002	556.2 ± 11.4	647.5 ± 6.3	1.76 ± 0.04
9	8	85	1.258 ± 0.002	539.0 ± 4.8	629.8 ± 3.9	1.90 ± 0.15
10	12	59	1.260 ± 0.004	528.2 ± 8.1	632.6 ± 3.9	1.86 ± 0.04
11	12	85	1.256 ± 0.001	542.3 ± 9.7	640.8 ± 6.8	1.97 ± 0.08
12	8	28	1.238 ± 0.003	532.0 ± 8.6	627.1 ± 7.4	2.24 ± 0.15
13	16	59	1.255 ± 0.003	533.7 ± 0.9	631.7 ± 2.5	1.88 ± 0.09
14	20	85	1.259 ± 0.001	529.4 ± 4.1	619.6 ± 3.2	1.80 ± 0.03
15	16	85	1.261 ± 0.002	533.7 ± 4.0	629.2 ± 5.4	1.93 ± 0.06

**Table 5.** AIC values evolution for each of the four response variables.

Model	AIC Values			
	Wire Diameter	Yield Strength	Tensile Strength	Uniform Elongation
M1	-176.3	440.3	382.4	15.7
M2	-176.4	437.8	377.2	13.8
M3	-182.9	437.3	383.7	14.1
M4	-183.4	434.1	378.4	11.9
M5	-218.9	390.5	344.6	-12.3
M6	-222.7	376.1	326.6	-18.2
M7	-245.1	374.0	345.1	-17.6
M8	-254.6	348.3	326.2	-25.0
M9	-264.6	335.6	321.8	-29.7
M10	-306.0	340.6	325.1	-23.2
M11	-369.6	<b>323.5</b>	320.1	-28.0
M12	<b>-390.8</b>	324.8	<b>318.9</b>	<b>-58.5</b>

**Table 6.** ANOVA results for the response variables.

Response Variable	Final Equation	P-value	R <sup>2</sup>	Adj. R <sup>2</sup>	CV	AP
Wire Diameter (mm)	$1.243 + 0.0053N - 0.0013N^2 + 0.000035D + 0.000000032D^2 - 0.000055ND + 0.000032N^2D + 0.00000013ND^2 - 0.00000021N^2D^2$	<0.0001	0.99	0.99	0.22	84.68
Yield Strength (MPa)	$525.50 - 1.35N + 0.82N^2 + 0.53D + 0.00089D^2 - 0.21ND - 0.0084N^2D + 0.0021ND^2$	<0.0001	0.96	0.95	1.41	25.99
Tensile Strength (MPa)	$582.35 + 7.46N + 0.019N^2 + 3.22D - 0.027D^2 - 0.57ND + 0.016N^2D + 0.0053ND^2 - 0.00018N^2D^2$	<0.0001	0.86	0.82	0.82	17.80
Uniform Elongation (%)	$-1.39 + 0.73N - 0.034N^2 + 0.15D - 0.0014D^2 - 0.029ND + 0.0012N^2D + 0.00025ND^2 - 0.000010N^2D^2$	<0.0001	0.91	0.88	6.11	17.06

**P:** probability of error; **R<sup>2</sup>:** coefficient of determination; **Adj. R<sup>2</sup>:** adjusted coefficient of determination; **CV:** coefficient of variation; **AP:** adequate precision.

and the response variables at the 5% probability level. The adjustment reliability is verified by using both the R<sup>2</sup> and adjusted R<sup>2</sup>. Within the models for each response variable, the lowest coefficient of determination was 86% and the highest 99%, i.e., the models explained at least 86% of the correlation between the variables involved.

The values of the adjusted coefficient of determination (adjusted R<sup>2</sup>) corroborated the AIC for choosing these selected models, presented in Table 6. An additional indication of the choice of models is in the AP criterion, of which, for all models it was noticed a value greater than four desirables<sup>26,31</sup>, thus indicating the suitability model to

the data. Furthermore, it was also noticed that the precision of experiments was high since the coefficient of variation (CV) was not greater than 10%<sup>32</sup>. Therefore, according to Table 6, all models are replicable since the CV values are well below this reference value.

The diagnostics plots, as predicted versus experimental values (Figure 3), complement the model's fit quality analysis. Furthermore, the graph points in Figure 3 are adjusted at an angle very close to the ideal, a straight line at 45°, which is desirable as it indicates substantial accordance between the actual data and the data obtained through the models.

Figure 4 presents four plots, one for each response variable studied, with the experimental points represented by the mean values and standard deviation (Table 4), and the curves of the final equations (Table 6) for each pulley D value used in the tests. All the experimental points in Figure 4 are fitted with their respective model curves, which

corroborates the results in Figure 3, showing that the models and the experimental points are in close agreement.

For model efficiency validation analysis, 3 experiments were conducted under different conditions to the initial tests (Table 7). As shown in Table 7, when comparing the results obtained by the model and with new tests, an average percentage error of 1.85% was obtained. This proves the capability of the models in Table 6 to estimate the values of the response variables in the range delimited by the proposed experimental design.

### 3.2. Process analysis

The response surface plots and contour plots are shown in Figures 5-6, respectively. The response surface plots for yield strength (Figure 5b) and tensile strength (Figure 5c) exhibit a valley region (red color), which indicates that the maximum stress relief conditions promoted by the Bauschinger effect

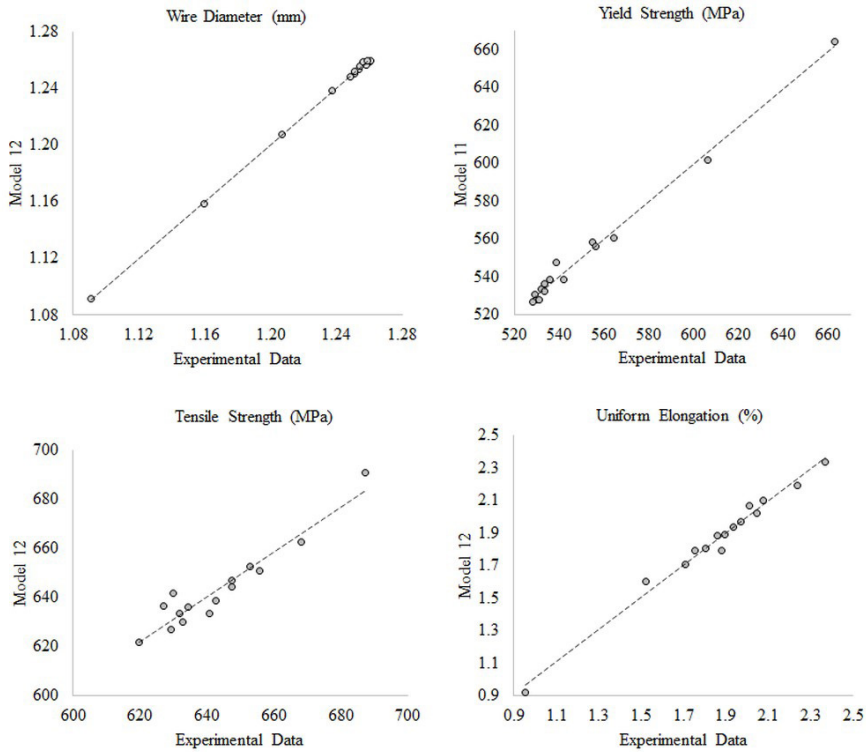


**Figure 3.** Plots of the model predicted values versus experimental values for (a) wire diameter (model 12), (b) yield strength (model 11), (c) tensile strength (model 12) e (d) uniform elongation (model 12).

**Table 7.** Validation experiment: model response versus new experimental results.

Conditions (D=35 mm)	After Cyclic Bending Testing Results											
	Wire Diameter (mm)			Yield strength (MPa)			Tensile Strength (MPa)			Uniform Elongation (%)		
Pulley Quantity	6	10	14	6	10	14	6	10	14	6	10	14
Experimental Result	1.255	1.244	1.221	523.8	522.9	560.7	623.9	616.4	632.0	2.14	2.12	1.89
Model Response	1.250	1.236	1.209	526.8	535.7	561.5	638.1	636.1	645.1	2.23	2.08	1.82
Error	-0.005	-0.008	-0.012	3.0	12.8	0.8	14.2	19.7	13.1	0.09	-0.04	-0.07
Percentual Error (%)	0.38	0.62	0.98	0.57	2.45	0.14	2.28	3.20	2.07	4.21	1.86	3.45
Standard Deviation	±0.001	±0.005	±0.002	±7.9	±3.5	±6.0	±5.1	±6.3	±1.1	±0.06	±0.10	±0.17

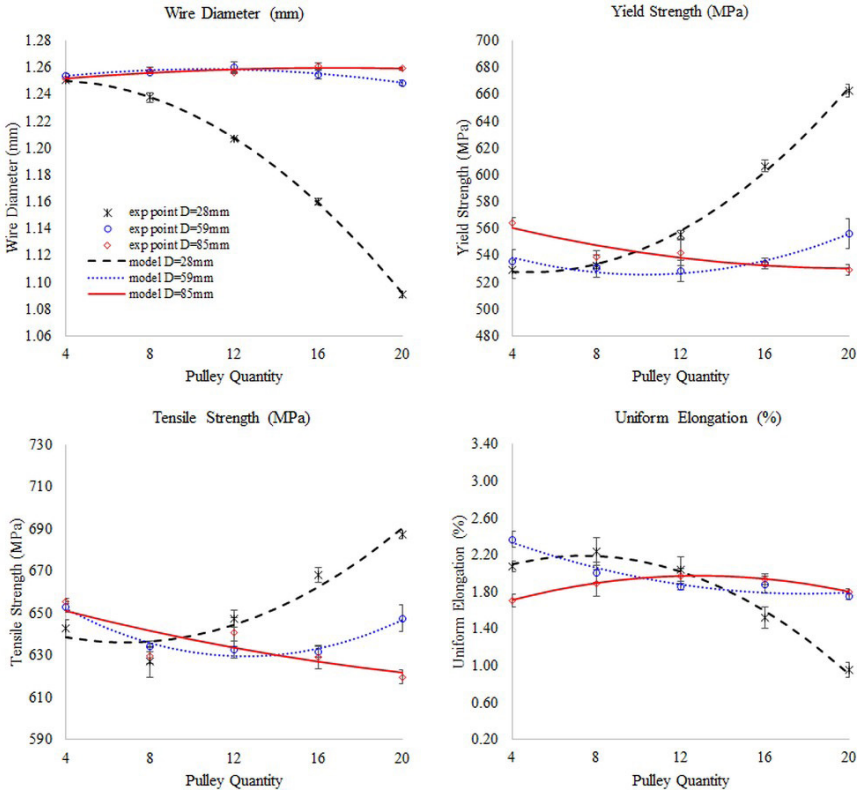


Figure 4. Plots of the model predicted curves versus experimental points for (a) wire diameter, (b) yield strength, (c) tensile strength e (d) uniform elongation.

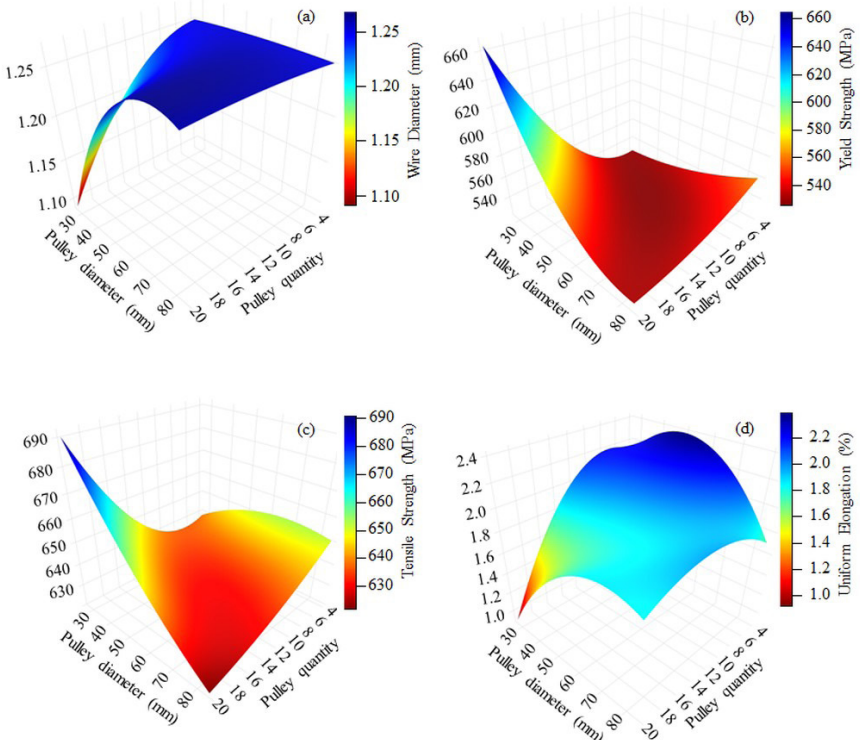


Figure 5. Response surface plots for (a) wire diameter, (b) yield strength, (c) tensile strength and (d) uniform elongation.

during cyclic bending is attributed to the number and diameter of pulleys in these spatial regions. Furthermore, both Figure 5b-5c show an asymmetric parabolic shape, with the presence of a valley region, which represents the space corresponding to the minimum values of the response variables. The tabs with more remarkable ascendancy (indigo/blue colors) correspond to the decreasing region of the wire diameter shown in Figure 5a. Pulleys less than 60 mm in diameter promote wire stretching during processing, as shown in Figure 5a, in the cyan, yellow, and red regions. Under these circumstances, there is a conflict between the hardening promoted by the strain hardening phenomenon and the softening produced by the Bauschinger effect during cyclic bending.

Regarding uniform elongation, the response surface plot (Figure 5d) shows a peak region in blue. In this region, the number and diameter of pulleys can produce the maximum plastic recovery during cyclic bending. Finally, analyzing the evolution of the wire diameter in Figure 5a, a blue threshold is highlighted, where the number and diameter of pulleys can be combined to keep the wire diameter unchanged after cyclic bending.

The bi-dimensional representation of the response variables (Figure 6) in the plane number/diameter of pulleys (contour plot) shows the isovalue lines that precisely delimit the mechanical property ranges. Thus, it is possible to precisely control the Bauschinger effect magnitude to change the tensile strength and plasticity of the ultra-low carbon steel within the desired range. For example, stress reliefs of 14% in yield strength are possible by cyclic bending using 12 pulleys of 59 mm diameter. Also, maximum recoveries of 103% in uniform elongation are achieved by cyclic bending with

4 pulleys of 50 mm diameter. These plastic recovery values corroborate with the typical range described by Enghag (2009), the reduction of the yield strength between 10% to 25% during cyclic bending<sup>2</sup>. Moreover, it becomes evident in Figure 6a that a critical diameter ( $D_c$ ) starting at 60 mm, where the addition of pulleys inside the CRD space, does not promote the wire stretching during the cyclic bending process.

### 3.3. Optimization analysis

Using the contour plots in Figure 6, finding the optimal condition for the metal stress relief is possible since this is the region where the Bauschinger effect magnitude is maximum to reduce the strength and recover the plasticity. To visualize this space graphically, the contour plots of yield strength, strength limit, and uniform elongation were superimposed on an overlay plot, shown in Figure 7.

Intersecting the isovalue lines, the shaded region was highlighted, indicating the area where the values of the response variables exhibit a better balance between plasticity gain and strength reduction. In addition, it is also possible to visualize the space where the operational conditions (number and diameter of pulleys) fit the shaded optimization criteria<sup>27</sup>.

An additional experiment was conducted by applying a condition from the optimum shaded region (OP Point: 10 pulleys of 59 mm diameter) to confirm the agreement between the results predicted by the models and those obtained from the experiments. As a result, as shown in Table 8, there is a close agreement in the softening capacity exhibited in the response variables obtained from the experiments and estimated by the models.

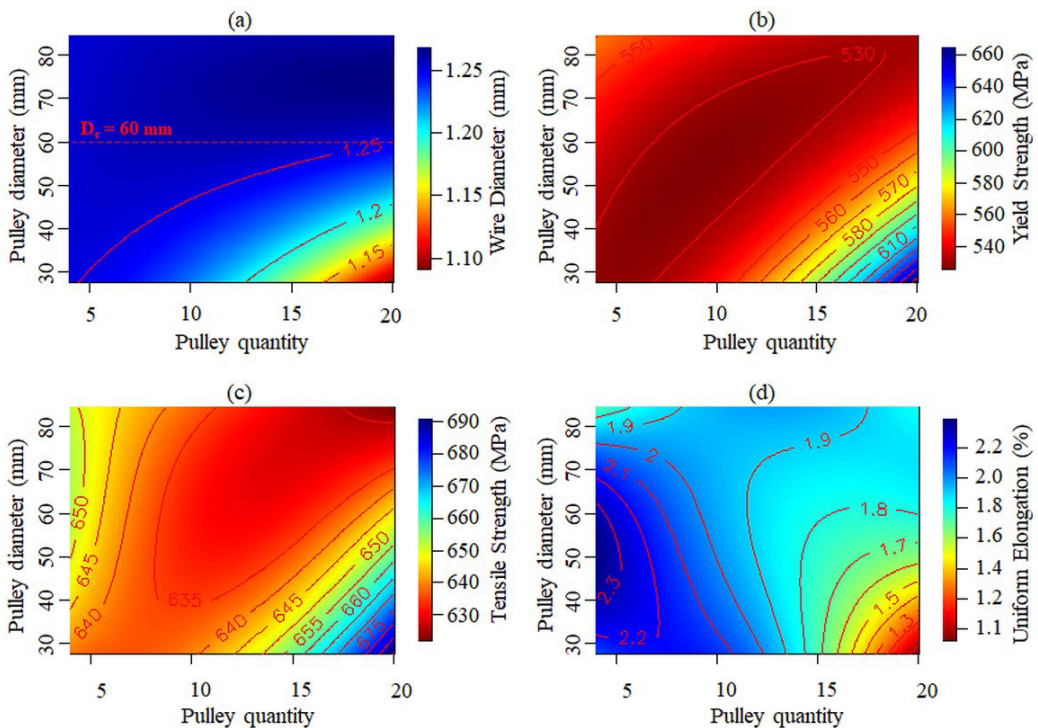
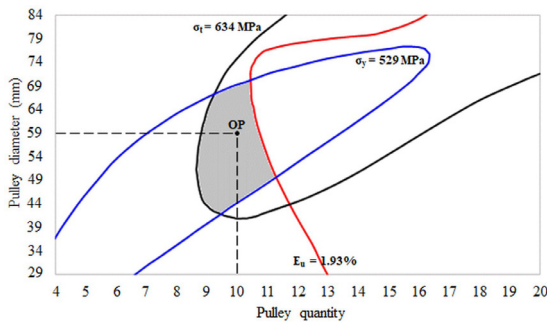


Figure 6. Contour plots for (a) wire diameter, (b) yield strength, (c) tensile strength and (d) uniform elongation.

**Table 8.** Optimum region verification experiment.

Conditions	After Cyclic Bending Testing Results			
	Wire Diameter (mm)	Yield Strength (MPa)	Tensile Strength (MPa)	Uniform Elongation (%)
OP = 10 pulleys with 59 mm diameter				
Experimental Result	1.254	523.6	627.8	1.88
Model Response	1.259	525.8	631.8	1.96
Error	0.005	2.2	4.0	0.08
Percentual Error (%)	0.37	0.42	0.63	4.46
Standard Deviation	±0.001	±4.9	±1.8	±0.17

**Figure 7.** Overlay plot for highlighting the optimal region of maximum softening.

## 4. Conclusions

This paper has aimed to present the experimental results issued from tests performed with an equipment designed to promote the Bauschinger effect, in ultra-low carbon steel wires, through alternated cyclic bending. As a result, it is possible to present the following conclusions:

- The alternated cyclic bending is effective in controlling the magnitude of the Bauschinger effect in ultra-low carbon steel wires;
- The cyclic bending can increase the uniform elongation and reduce the strength, in a controlled way, in ultra-low carbon steel wires;
- The results showed that with the application of Akaike Information Criterion (AIC), it was possible to obtain regression models which showed satisfactory agreement between the experimental results and predicted results from the general equations;
- The surface and contour plots showed the correlation between the operational conditions of cyclic bending and the modification of the strength/plasticity of the ultra-low carbon steel, allowing to navigate in the defined space in order to find the most suitable operational parameters available;
- The overlay plot showed the optimal condition region that exhibits the equilibrium between plasticity gain and strength reduction. For the tested condition in the optimum region using 10 pulleys of 59 mm diameter, 67% gain in elongation and 14% reduction in yield strength were obtained.

## 5. Acknowledgements

To the Federal University of Ouro Preto (UFOP) postgraduate program - REDEMAT and the Federal Institute of Education Science and Technology of Minas Gerais (IFMG).

## 6. References

1. Amine K, Larsson J, Pejryd L. Experimental comparison of roller die and conventional wire drawing. *J Mater Process Technol.* 2018;257:7-14.
2. Enghag P. Steel wire technology. Örebro: Applied Materials Technology; 2009.
3. Boger RK, Wagoner RH, Barlat F, Lee MG, Chung K. Continuous, large strain, tension/compression testing of sheet material. *Int J Plast.* 2005;21:2319-43.
4. Buciumeanu M, Palaghian L, Miranda AS, Silva FS. Fatigue life predictions including the Bauschinger effect. *Int J Fatigue.* 2010;33:145-52.
5. Chen B, Hu JN, Wang YQ, Zhang SY, Van Petegem S, Cocks ACF et al. Role of the misfit stress between grains in the Bauschinger effect for a polycrystalline material. *Acta Mater.* 2014;85:229-42.
6. Ellermann A, Scholtes B. The Bauschinger effect in different heat treatment conditions of 42CrMo4. *Int J Struct Changes Sol.* 2011;3:1-13.
7. Figueiredo RB, Corrêa ECS, Monteiro WA, Aguilar MTP, Cetlin PR. The effect of cyclic bending on the mechanical properties and dislocation structures of drawn steel bars. *J Mater Sci.* 2009;45:804-10.
8. Hemmerich E, Rolfe B, Hodgson PD, Weiss M. The effect of pre-strain on the material behaviour and the Bauschinger effect in the bending of hot rolled and aged steel. *Mater Sci Eng A.* 2010;528:3302-9.
9. Kim DW, Kim W-K, Bae J-H, Choi W-D, Kim HS, Lee S. Yield-strength prediction of flattened steel pipes by competing Bauschinger effect and strain hardening during pipe-forming. *Sci Rep.* 2019;9:1-11.
10. Alexandrov S, Lyamina E, Aoh JN, Jeng YR. Description of residual stresses in autofrettaged open-ended cylinders made of high-strength steel. *Materials.* 2020;13(3):2940.
11. Yoshida F, Uemori T, Fujiwara K. Elastic-plastic behavior of steel sheets under in-plane cyclic tension-compression at large strain. *Int J Plast.* 2002;18:633-59.
12. Harjo S, Kubota S, Gong W, Kawasaki T, Gao S. Neutron diffraction monitoring of ductile cast iron under cyclic tension-compression. *Acta Mater.* 2020;196:584-94.
13. Toribio J, Kharin V, Ayaso FJ, Lorenzo M, González B, Matos JC et al. Analysis of the Bauschinger effect in cold drawn pearlitic steels. *Metals.* 2020;10:1-14.

14. Liu D, He Y, Shen L, Lei J, Guo S, Peng K. Accounting for the recoverable plasticity and size effect in the cyclic torsion of thin metallic wires using strain gradient plasticity. *Mater Sci Eng A*. 2015;647:84-90.
15. Elliot RA, Orowan E, Udoguchi T, Argon AS. Absence of yield points in iron on strain reversal after aging, and the Bauschinger overshoot. *Mech Mater*. 2004;36:1143-53.
16. Correa ECS, Aguilar MTP, Silva EMP, Cetlin PR. The effect of sequential tensile and cyclic torsion straining on work hardening of steel and brass. *J Mater Process Technol*. 2003;142:282-8.
17. Schilli S, Seifert T, Kreins M, Krupp U. Bauschinger effect and latent hardening under cyclic micro-bending of Ni-base Alloy 718 single crystals: part II. Single crystal plasticity modeling with latent kinematic hardening. *Mater Sci Eng A*. 2022;830:1-19.
18. Ha J, Lee MG, Barlat F. Strain hardening response and modeling of EDDQ and DP780 steel sheet under non-linear strain path. *Mech Mater*. 2013;64:11-26.
19. Verma RK, Kuwabara T, Chung K, Haldar A. Experimental evaluation and constitutive modeling of non-proportional deformation for asymmetric steels. *Int J Plast*. 2010;27:82-101.
20. Tarigopula V, Hopperstad OS, Langseth M, Clausen AH. Elastic-plastic behaviour of dual-phase, high-strength steel under strain-path changes. *Eur J Mech A, Solids*. 2008;27:764-82.
21. Akaike H. Information theory as an extension of the maximum likelihood principle. In: *Second International Symposium on Information Theory*; 1971 Sep 2-8; Tsakhkadzor. Proceedings. Budapest: Akademiai Kiado; 1973. p. 267-81.
22. Snipes M, Taylor DC. Model selection and Akaike information criteria: an example from wine ratings and prices. *Wine Econ Policy*. 2014;3:1-7.
23. Montgomery DC. *Design and analysis of experiments*. Phoenix: John Wiley & Sons; 2017.
24. Dieter GE. *Mechanical metallurgy*. Tokyo: McGraw-Hill; 1976.
25. Montgomery DC, Runger GC. *Applied statistics and probability for engineers*. Hoboken: Wiley; 2018.
26. Noordin MY, Venkatesh VC, Sharif S, Elting S, Abdullah A. Application of response surface methodology in describing the performance of coated carbide tools when turning AISI 1045 steel. *J Mater Process Technol*. 2003;145:46-58.
27. Ghafari S, Aziz HA, Isa MH, Zinatizadeh AA. Application of response surface methodology (RSM) to optimize coagulation–flocculation treatment of leachate using poly-aluminum chloride (PAC) and alum. *J Hazard Mater*. 2008;163:650-6.
28. R Core Team. *R: a language and environment for statistical computing*. Vienna: R Foundation for Statistical Computing; 2022.
29. Lawson J. *Design and analysis of experiments with R*. Boca Raton: CRC Press; 2015.
30. Hinkelmann K, Kempthorne O. *Design and analysis of experiments*. Hoboken: John Wiley & Sons; 2008.
31. Dharma S, Masjuki HH, Ong HC, Sebayang AH, Silitonga AS, Kusumo F et al. Optimization of biodiesel production process for mixed *Jatropha curcas*–*Ceiba pentandra* biodiesel using response surface methodology. *Energy Convers Manage*. 2016;115:178-90.
32. Beg QK, Sahai V, Gupta R. Statistical media optimization and alkaline protease production from *Bacillus mojavenensis* in a bioreactor. *Process Biochem*. 2003;39:203-9.